Supporting Information for

Air-Sea Turbulent Heat Flux Feedback over Mesoscale Eddies

Sophia Moreton [1], David Ferreira [1], Malcolm Roberts [2], Helene Hewitt [2]

1. University of Reading, UK

2. Met Office Hadley Centre, Exeter, UK

Contents of this file

Introduction

This supporting information provides more details of the filtering and composite averaging method, additional figures and a table of the number of eddy snapshots for each amplitude bin.

Text S1.

Filtering and composite averaging method

The high-pass filtered field is constructed by removing a low-passed field obtained from a Gaussian filtering of 20^0 zonally and 10^0 meridionally. The type of the filtering is important as it can change the strength of the anomaly within an eddy, and our approach differs from previous work e.g. Hausmann et al., (2012) and Frenger et al. (2013). We maintain a consistent strength of filtering across resolutions and variables, as well as for a regular and irregular NEMO grid, by applying grid point-dependent filtering.

Composite averaging includes for all eddies globally over one year, to effectively remove variability associated with changing oceanic and atmospheric conditions. The centre of the eddy is identified by the algorithm. A region around the eddy, 2.8 times the effective eddy radius (L_{eff}), is selected by identifying the nearest grid point to the eddy centre on either the ocean or atmospheric grid from the fields (THF, T_{air}, SST_O and SST_A). The 5.6 x 5.6 L_{eff} patch of a high-pass filtered variable (e.g. SST) is then extracted and normalized by L_{eff} in zonal and meridional directions. For ocean variables, interpolating the high-pass filtered patch to a high resolution grid converts from the irregular NEMO grid to a regular grid. The selected year of data for compositing for each model configuration is 4 or 5 years after the eddy tracking began in 1950 (or 1970 for N216-12):

> N216_025 : 1955
> N512_12 : 1954
> N216_12 : 1975

For the results used in this study, rotating the snapshots before composite averaging made little difference. However when separating the eddies in each hemisphere a poleward shift can be observed in anticyclones, or an equatorward shift in cyclones, between the eddy centre and the maximum SST_O (or LHF) anomaly. By separating each hemisphere, this effectively produces a background northward SST gradient in the Northern Hemisphere, and a background southward SST gradient in the Southern Hemisphere. The phase shift, which can be observed in each model resolution, is consistent with observations and can be amplified in smaller amplitude eddies, where the monopole spatial structure changes to a dipole (Hausmann et al, 2012).

According to Hausmann et al., 2012 (their Appendix A), 2503 snapshots (averaged across all amplitudes and model resolutions) is enough to remove weather noise and obtain a robust average. It should be highlighted that, in the present study, the number of snapshots in the larger amplitude bins are far fewer, down to about 250 snapshots. The number of eddy snapshots used in each bin can be found in TableS1 below.

Assuming a normal distribution of data and using the student's t-test, 95% confidence intervals are supplied in Fig. 2 and 3 to find the confidence of the fitted linear regression line.

References
Hausmann U. and Czaja A., 2012, The observed signature of mesoscale eddies in sea surface temperature and the associated heat transport, Deep Sea Research Part 1: Oceanographic Research Papers, 70, 60-72, doi: 10.1016/j.dsr.2012.08.005
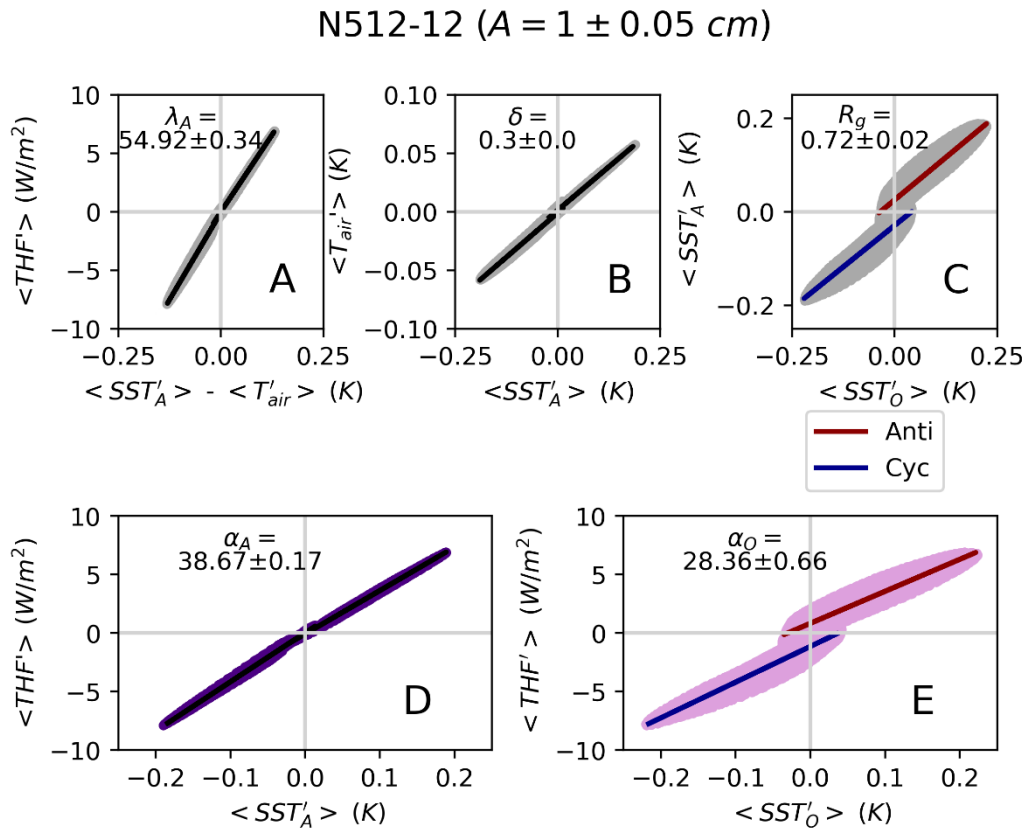
Figure S1. A repeat of Fig 2 for the smallest amplitude eddies from N512-12. Anticyclonic eddies are separated from cyclonic eddies due to different regression lines and plotted in red and blue, respectively.
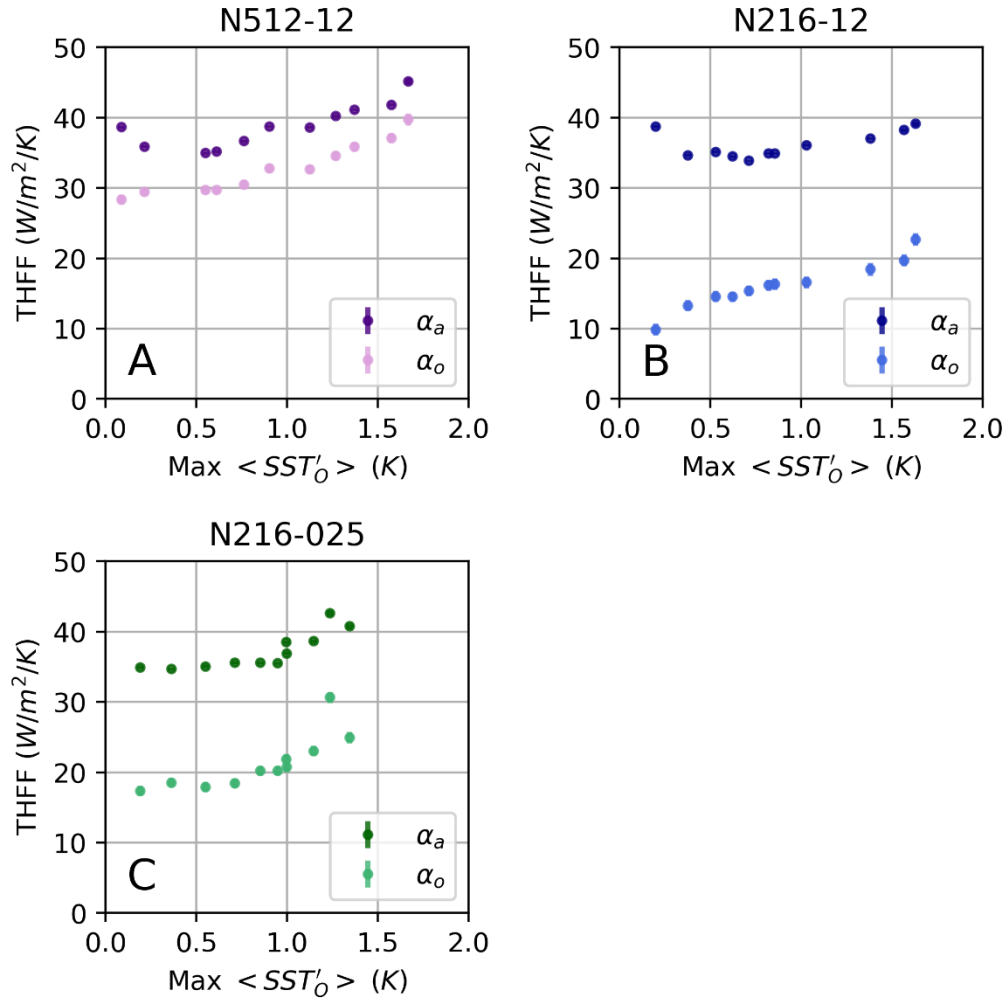
Figure S2. A repeat of Fig 3 plotting α_O and α_A as a function of the maximum SST_O anomaly, instead of eddy amplitude, for each configuration: N512-12, N216-12, and N216-025.
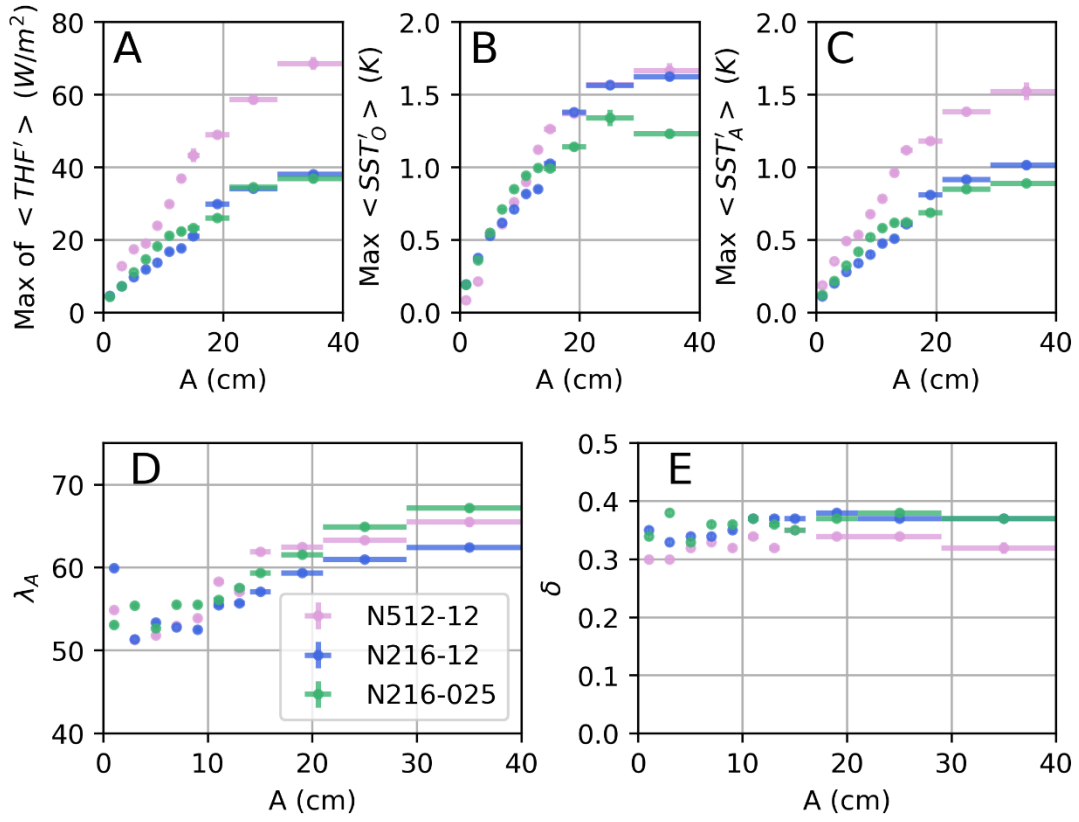
Figure S3. Scatter plots of (A) the maximum absolute THF (in W m^{-2}), (B) SST_O (in K) and (C) SST_A (in K) eddy composites, λ_A (D) and δ (E) for each binned eddy amplitude (A, in cm). Results are shown for each configuration: N512-12, N216-12, and N216-025.
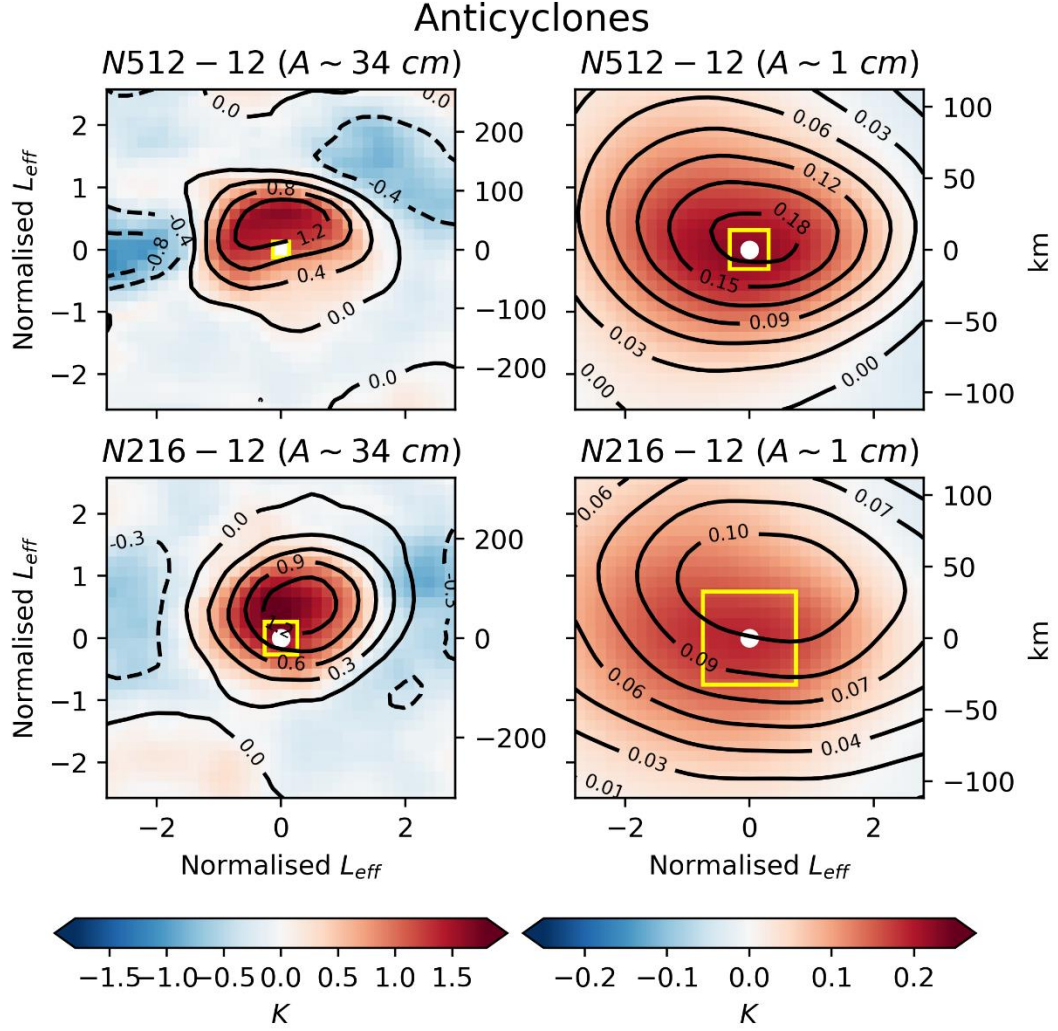
Figure S4. Composite maps of anti-cyclonic eddies with SST_O (colour) and SST_A (contours) anomalies (in K) for the large amplitude (A=34+/-6 cm) eddies (left) and the small amplitude (A=1+/-0.05 cm) eddies (right). Results for the N512-12 and N216-12 configurations are shown in the upper and lower rows, respectively. The yellow square represents the approximate horizontal grid resolution in the atmosphere at the mid-latitudes.

Amp	N216-025 (A)	N216-025 (C)	N216-12 (A)	N216-12 (C)	N512-12(A)	N512-12 (C)
1±0.05	5878	3228	8492	4487	10506	4992
3±0.05	5051	4300	6732	6084	5857	5734
5±0.05	1891	2232	2555	2998	1709	2367
7±0.1	1579	2142	2215	3119	1132	2021
9±0.2	1513	2142	2122	3158	1020	1793
11±0.5	1773	3440	2582	4702	1118	2254
13±0.5	1153	1926	1458	2799	715	1349
15±1	1254	2546	1909	3556	857	1704
19±2	1212	2151	1537	2858	847	1308
25±4	697	1934	1224	2427	502	1062
34±6	568	799	498	1355	248	257

Table S1. Number of eddy snapshots for each eddy amplitude bin (Amp) in cm, for each model resolution and polarity (anticyclonic, A or cyclonic, C).